

# Generation of a tendon-like tissue from human iPSC cells

Journal of Tissue Engineering  
Volume 13: 1–13  
© The Author(s) 2022  
Article reuse guidelines:  
sagepub.com/journals-permissions  
DOI: 10.1177/20417314221074018  
journals.sagepub.com/home/tej



Hiroki Tsutsumi<sup>1</sup>, Ryota Kurimoto<sup>1</sup>, Ryo Nakamichi<sup>2</sup>, Tomoki Chiba<sup>1</sup>, Takahide Matsushima<sup>1</sup>, Yuta Fujii<sup>1</sup>, Risa Sanada<sup>1</sup>, Tomomi Kato<sup>1</sup>, Kana Shishido<sup>1</sup>, Yuriko Sakamaki<sup>3</sup>, Tsuyoshi Kimura<sup>4</sup>, Akio Kishida<sup>4</sup> and Hiroshi Asahara<sup>1,2</sup> 

## Abstract

Tendons and ligaments are essential connective tissues that connect the muscle and bone. Their recovery from injuries is known to be poor, highlighting the crucial need for an effective therapy. A few reports have described the development of artificial ligaments with sufficient strength from human cells. In this study, we successfully generated a tendon-like tissue (bio-tendon) using human induced pluripotent stem cells (iPSCs). We first differentiated human iPSCs into mesenchymal stem cells (iPSC-MSCs) and transfected them with Mohawk (Mkx) to obtain Mkx-iPSC-MSCs, which were applied to a newly designed chamber with a mechanical stretch incubation system. The embedded Mkx-iPSC-MSCs created bio-tendons and exhibited an aligned extracellular matrix structure. Transplantation of the bio-tendons into a mouse Achilles tendon rupture model showed host-derived cell infiltration with improved histological score and biomechanical properties. Taken together, the bio-tendon generated in this study has potential clinical applications for tendon/ligament-related injuries and diseases.

## Keywords

Mohawk (Mkx), tendon, tissue engineering, mechanical-stress, iPSC cell

Date received: 14 October 2021; accepted: 1 January 2022

## Introduction

Tendons connect muscles and bones, and ligaments connect two bones. Both these tissues are critical for transmitting and stabilizing the force produced by muscles and facilitating joint movements.<sup>1</sup> Tendon injuries may cause joint motion disability and reduced quality of life.<sup>2</sup> There are several treatment options for tendon injuries, including surgical repair or conservative approaches; however, complete cure is difficult and may take time because tendons have low repair capacity, owing to low cell density, and poor innervated blood vessels.<sup>3</sup> For instance, Achilles tendon rupture is a frequent tendon injury occurring in 6%–18% of athletes each year and reportedly affects approximately 1 million patients per year in the United States. Once injured, it takes approximately 6 months to return to work.<sup>4</sup>

Pharmacological approaches and cell transplantation strategies using stem and progenitor cells are under development,<sup>5</sup> but their medical application is yet not established.<sup>6</sup>

<sup>1</sup>Department of Systems BioMedicine, Tokyo Medical and Dental University, Bunkyo City, Japan

<sup>2</sup>Department of Molecular Medicine, The Scripps Research Institute, La Jolla, CA, USA

<sup>3</sup>Research Core, Tokyo Medical and Dental University, Bunkyo City, Japan

<sup>4</sup>Department of Material-Based Medical Engineering, Tokyo Medical and Dental University, Bunkyo City, Japan

### Corresponding author:

Hiroshi Asahara, Department of Systems BioMedicine, Tokyo Medical and Dental University, 1-5-45, Yushima, Bunkyo City, Tokyo 113-8510, Japan.

Email: asahara.syst@tmd.ac.jp



Autologous or allogeneic tendons for tendon reconstruction have routinely been applied for medical treatment and have shown relatively good outcomes; however, these materials encounter several problems. Autologous tendon transplantation raises concerns about complications such as pain and nerve damage during graft harvesting.<sup>7</sup> When allogeneic or xenogeneic tendons are used, decellularization processes are performed to lower their immunogenic effects.<sup>8</sup> However, transplantation of xenogeneic tendons may not completely eliminate immunogenicity.<sup>9</sup> As for allogeneic tendons, the supply of tissues is limited. Artificial tendons made of polyester and other materials have sufficient tensile strength in the early phase; however, they are not replaced into the recipient tissue; thus, the transplanted material often collapse in the long run.<sup>10</sup> In addition, the risk of allergy and infection with artificial materials could also pose problems.<sup>11</sup> Dermis-derived tissues have been applied for tendon reconstruction surgery, but their collagen composition and tissue structure differ from those of tendons.<sup>12</sup> Moreover, these tissues could not recruit tendon stem/progenitor cells to reconstruct the tendon tissue with proper tendinous matrix formation.<sup>13</sup> Based on these facts, an ideal medical strategy to reconstruct tendon ruptures would involve development of an artificial tendon-like tissue with tendon-like mechanical and histological properties from human tendon cells *in vitro*.

We have previously reported that mouse mesenchymal stem cells overexpressing Mohawk (Mkx) could form a tendon-like tissue in a three-dimensional (3D) cyclic stretch culture system.<sup>14</sup> In the present study, we significantly improved the cell stretch chamber system to enable the production of enlarged and well-structured bio-tendons from human induced pluripotent stem cell (iPSC)-mesenchymal stem cells (MSCs) overexpressing Mkx. Aside from the fact that the tissues are derived from human cells, the decellularization process of the bio-tendons should reduce the risk of tumorigenesis and immune reactions associated with the use of allogeneic iPSCs. In fact, we observed significantly improved tendon reconstruction using the newly developed bio-tendon transplant in a mouse tendon rupture model through histological and biomechanical evaluations. Our results support the potential of this bio-tendon for clinical applications.

## Methods

### *iPSC-MSC differentiation and maintenance*

Induction of differentiation of induced pluripotent stem cells (iPSCs) into iPSC-mesenchymal stem cells (MSCs) was performed according to a previous report<sup>15</sup> with some modifications. The iPSC line 253G1 was maintained on a 10cm dish coated with Geltrex (Life Technologies, CA,

United States) in Essential 8 (E8) medium (Life Technologies, CA, United States). iPSCs were plated onto Geltrex-coated dishes in E8 medium with 10  $\mu$ M Y-27632 (BioVision, CA, United States) and cultured for 2 additional days in a differentiation medium comprising 10 ng/mL basic fibroblast growth factor (FGF; R&D Systems, MN, USA), 4  $\mu$ M SB431542 (Stemgent, MA, United States), and 4  $\mu$ M WNT agonist CHIR99021 (CHIR) (Stemgent) in Essential 6 (E6) medium (Life Technologies). Differentiation medium was daily changed for 5 days. On day 6, differentiated neural crest cells (NCCs) were plated on a Geltrex-coated dish in mesenchymal stem cell (MSC) culture media (MEM $\alpha$  + 10% fetal bovine serum [FBS] + 1% penicillin-streptomycin + 1 [v/v%] 100 $\times$  non-essential amino acid solution [NEAA; Gibco], 1 [v/v%] 100 $\times$  GlutaMAX [Gibco]). After three passages, the surface coating was switched from Geltrex to 1% gelatin (Wako, Osaka, Japan) to support iPSC-MSC adhesion and growth. To establish stable Mkx and GFP expression, iPSC-MSCs were infected with a suitable lentivirus. Stable cell lines were established using 1  $\mu$ g/mL puromycin (InvivoGen, CA, United States) for 3 days.

### *3D-cultures*

Established Mkx-iPSC-MSCs or GFP-iPSC-MSCs were embedded in a 3D-culture cocktail. The 3D-culture cocktail was constructed by mixing collagen gel (final concentrations: 2 mg/mL Cellmatrix (Type I-A, Nitta Gelatin Inc., Osaka, Japan) and 1 $\times$  collagen neutralization buffer (Type I-A, Nitta Gelatin Inc.)), pro-survival cocktail final concentrations: 100 nM B-cell lymphoma extra-large (Bcl-XL) BH4 4-23 (197217-1MG, Calbiochem, CA, United States), 100  $\mu$ M carbobenzoxy-valyl-alanyl-aspartyl-[O-methyl]-fluoromethylketone (Z-VAD-FMK) (Promega, WI, United States), 200 ng/mL LongR3 insulin-like growth factor 1 (IGF-1) (PeproTech, NJ, United States), and 100  $\mu$ M pinacidil monohydrate (ChemCruz, TX, United States), and MSC culture media.

The 3D chamber was coated with 1% gelatin and incubated at 37°C and 5% CO<sub>2</sub> for 30 min. After washing thrice with 1 $\times$  phosphate-buffered saline (PBS), 2.0 $\times$ 10<sup>6</sup> cells were transferred to a 3D-culture cocktail mixture and incubated at 37°C and 5% CO<sub>2</sub> for 60 min for gelation. Following gelation, the culture medium was added to the chamber.

### *Mechanical stimulation*

Following 24 h incubation, the 3D-cultured samples were set into a mechanical cell stretch system device (Shellpa Pro, Menicon Co., Ltd./Life Science Department, Aichi, Japan). Cyclic mechanical stretch was performed for 2 weeks by gradually increasing the stretch loading rate as follows: 1% (day 1), 2% (day 2), 3% (day 3), 4% (day 4), and 5% (day 5–14). The cyclic mechanical stretch was programed at 0.25 Hz for 18 h/day, followed by resting for

6 h/day at 37°C and 5% CO<sub>2</sub>. Daily medium changes were also required.

### ***Decellularization by HHP, DNase treatment, and chemical treatment***

The cultured bio-tendon was placed into a plastic pack filled with saline and sealed to prevent implosion and leakage during the procedure. The pack was then pressurized at 1000 MPa at 30°C for 10 min using an HHP machine (Dr. CHEF; Kobe Steel, Ltd., Hyogo, Japan). After pressurization, the bio-tendon was incubated with a DNase buffer (Takara, Tokyo, Japan) containing 0.4 U/mL recombinant DNase solution (Roche Diagnostics, Tokyo, Japan) for 24 h at 4°C. After incubation, the bio-tendon was washed thrice with 30% ethanol (EtOH) by continuous shaking for 5 min at each step. Finally, 1-ethyl-3-(3-Dimethylaminopropyl) carbodiimide (EDC)/N-hydroxysuccinimide (NHS)-based cross-linking was performed by adding 70 mM EDC (Wako, Osaka, Japan) and 70 mM NHS (Wako, Osaka, Japan) with 30% EtOH for 24 h at 4°C. The processed bio-tendon was incubated in 1× phosphate-buffered saline (PBS) at 4°C until the experiment.

### ***Flow cytometry***

Differentiation of iPSC-MSCs was characterized using flow cytometry. Cells were harvested using 0.25% trypsin and quenched by adding MEM $\alpha$  medium containing 10 v/v% FBS. After washing with PBS, the cells were incubated for 60 min on ice with fluorescent-conjugated antibodies against CD44, CD73, CD90, and CD105 (R&D Systems) using a fluorescence-activated cell sorting (FACS) buffer (PBS containing 1 [v/v%] FBS). The labeled cells were analyzed using a BD Calibur flow cytometer.

### ***RNA isolation and qRT-PCR***

Total RNA was extracted using TRIzol reagent (Invitrogen, Grand Island, NY, USA). PrimeScript RT reagent Kit (Takara, Tokyo, Japan) was used for reverse transcription of mRNA. Complementary DNA was quantitated by qRT-PCR using a Thunderbird SYBR mix (Toyobo Co., Osaka, Japan). *Actb* expression served as a control for mRNA expression<sup>16,17</sup> and the changes in gene expression were quantified using the  $\Delta$ CT and  $\Delta\Delta$ CT method.

### ***Histological and immunohistochemical analyses***

Tissue samples were fixed in 4% paraformaldehyde for overnight at 4°C, washed in 1× PBS, cryo-preserved in 20% sucrose for overnight, and embedded in optimal cutting temperature (OCT) compound (45833, Sakura

Finetek Japan Co., Ltd., Tokyo, Japan). Then, the bio-tendon was cryo-sectioned at 10  $\mu$ m thickness and desiccated by air-drying for overnight. Histological staining was performed using hematoxylin (131-09665, FUJIFILM Wako Pure Chemical Corp.) and eosin (051-06515, FUJIFILM Wako Pure Chemical Corp.), Picosirius red staining kit (24901-500, Polysciences, Inc., PA, United States), and Elastica Van Gieson (EVG) staining kit (1.15974.0002, Merck Millipore, Burlington, MA, USA) according to the manufacturer's instructions.

### ***RNA-sequencing (RNA-seq)***

RNA-seq libraries were prepared by removing rRNA with using rRNA-depletion kit (NEB, E6310) and directional library synthesis kit (NEB, E7420). RNA libraries were sequenced by NextSeq500 High-output kit. Mapping fastq data and calculating the expression of each gene Adapters in Fastq files were trimmed using TrimGalore software ([https://www.bioinformatics.babraham.ac.uk/projects/trim\\_galore/](https://www.bioinformatics.babraham.ac.uk/projects/trim_galore/)). Fastq files were mapped to human genomes (hg19) using STAR software<sup>18</sup> (<https://github.com/alexdobin/STAR>), and the amount of each transcript was calculated with RSEM software<sup>19</sup> (<https://github.com/deweylab/RSEM>). Extracting differently expressed genes on iDEP.93. The counted data was transformed with EdgeR (log<sub>2</sub> (CPM (counts per million) + 4)), and volcano plot was generated. All of these steps were performed by iDEP.93<sup>20</sup> (<http://bioinformatics.sdstate.edu/idep93/>). The raw data of RNA-seq were deposited in the GEO under accession number GSEXXXXX (GSE No. will be delivered soon).

### ***Electron microscopy***

Tendon/ligament-like tissues were dissected and fixed in 2.5% glutaraldehyde in 0.1 M phosphate buffer (PB) overnight. For scanning electron microscopy (SEM), the specimens were dried in a critical-point drying apparatus (HCP-2, Hitachi, Ltd.) with liquid CO<sub>2</sub> and were sputter-coated with platinum. Then, the specimens were observed using SEM (S-4500, Hitachi, Ltd.). We evaluated two samples in each specimen. Three sections from each sample were randomly selected and analyzed.

### ***Stretch test***

The mechanical properties were measured using a creep meter (RE-3305S, Yamaden, Tokyo, Japan). After measuring the initial length (mm), diameter (mm), and thickness (mm) using a micrometer, the samples were fixed with two grips, which were pulled at a constant speed of 0.05 mm/s until failure, and the tensile strength (N) and failure strain (mm) was measured. We calculated cross-sectional area

(mm<sup>2</sup>) using initial diameter and thickness. The stiffness was manually determined from the slope in the linear region of the failure-stress curve.

The tensile strength (MPa), failure strain (%), stiffness, and Young's modulus were calculated using the following formulas:

$$\text{Tensile strength (MPa)} = \frac{\text{tensile strength (N)}}{\text{cross-sectional area (mm}^2\text{)}}.$$

$$\text{Failure strain (\%)} = \frac{\text{failure strain (mm)}}{\text{initial length (mm)}}.$$

$$\text{Stiffness} = \frac{\text{Stress (N)}}{\text{Strain (mm)}}.$$

$$\text{Young's modulus} = \frac{\text{stiffness} \times \text{initial length (mm)}}{\text{cross-sectional area (mm}^2\text{)}}.$$

### Transplantation

For histological analysis, 8- to 10-week-old male mTmG mice (JAX stock #007676) were anesthetized. Under aseptic conditions, approximately 5 mm wide resections were bilaterally made in the Achilles tendons. The processed bio-tendon was transplanted between the gaps using an 8-0 nylon suture. As a control, pepsin-solubilized collagen (Type I-C, Nitta Gelatin Inc., Osaka, Japan) was injected into the gap. The stretch test sample was unilaterally transplanted.

### Quantitative assessment of histological analysis

We analyzed fiber alignment, fiber structure, nuclear roundness, and inflammation referring to a grading system in previous studies.<sup>21</sup> These four parameters were quantified by two blinded observers using 0–3 grading scores as follows: 0 (normal), 1 (slightly abnormal), 2 (moderately abnormal), and 3 (severely abnormal). Detailed information on the histological score is described in Table 1.

### Statistical analysis

All values are presented as mean  $\pm$  SEM. Statistically significant differences were assessed by unpaired two-tailed Student's *t*-test and one-way analysis of variance (ANOVA) with Tukey's post hoc test. Statistical significance was set at  $p < 0.05$ . Gene expression ( $n = 3$ ), stretch test of bio-tendon (GFP-bio-tendon;  $n = 6$ , Mkx-bio-tendon;  $n = 7$ ), histology analysis ( $n = 3$ – $5$ ), and stretch test of post-transplant samples (intact,  $n = 10$ ; gel,  $n = 10$ ; GFP-bio-tendon,  $n = 10$ ; Mkx-bio-tendon,  $n = 9$ ) were analyzed at each time point. All bio-tendons had different replicates derived from different 3D cultures. The inter-observer correlation

of the quantitative assessment of histological analysis was 0.835. The power of total histological score in 6-week post-transplantation samples was 0.971 in post hoc power analysis using G\*Power software.<sup>22</sup>

## Results

### Differentiation of iPS cells into iPSC-MSCs and enhancement of tendon-related gene expression by Mkx overexpression

As an ideal source to produce an artificial tendon tissue, we utilized human iPS cells that exhibit pluripotency and proliferative capacity<sup>23</sup> (Figure 1(a)) and could express human matrix genes. Based on previous findings<sup>24–27</sup> that Mkx could differentiate MSCs into tendon-like cells, we first prepared human MSCs derived from human iPSCs (iPSC-MSCs) via neural crest cells (NCCs) as previously described.<sup>15</sup> We confirmed that iPSC-MSCs showed spindle-shape morphology and expressed MSC specific antigen (Supplemental Figure 1). Also, we observed higher expression of CD44, CD73, and CD105 in iPSC-MSCs than in iPSCs by RNA-seq (Supplemental Figure 2). iPSC-MSCs were induced to overexpress Mkx or green fluorescent protein (GFP) using a lentivirus system (thereafter we referred to Mkx-iPSC-MSCs and GFP-iPSC-MSCs, respectively.) We detected elevated expression of *Scx* in GFP-iPSC-MSCs, however the expression of *Scx* was low compared with Mkx and no significant changes in the expression of another tendon-related genes, such as *Colla1*, and *Col3a1* and *Fmod* (Supplemental Fig 3). As GFP had advantages in monitoring the efficiency of lentivirus infection, we chose GFP-iPSC-MSCs as a control. Consistent with previous reports,<sup>24</sup> Mkx-iPSC-MSCs showed a sharp tendon cell-like morphology, but GFP-iPSC-MSCs did not exhibit any change in their shape (Figure 1(b)). The expression of tendon-related genes, including *Scx*, *Colla1*, *Col3a1*, *Dcn*, and *Fmod* was upregulated in Mkx-iPSC-MSCs, but not in GFP-iPSC-MSCs<sup>27,28</sup> (Figure 1(c)), indicating that Mkx-iPSC-MSCs exhibited tendon cell properties and tendon-specific gene expression.

### Preparation of Mkx-iPSC-MSC–derived artificial tendons using a new chamber

To produce artificial tendons of sufficient size from Mkx-iPSC-MSCs, we improved the cyclic stretching 3D culture system<sup>14</sup> by developing a novel stretching culture chamber where an artificial tendon was placed on both sides to stably apply the propagation stimulus (Figure 1(a), Supplemental Figure 4).

GFP-iPSC-MSCs and Mkx-iPSC-MSCs were cultured in 3D stretch cultures for 15 days to create artificial tendon-like tissues (bio-tendons) with uniform thickness (Figure 2(a)). We applied 5% stimulation because this was

**Table 1.** Histology score.

	0	1	2	3
Fiber structure	continue, long fiber	Slightly fragmented	Moderately fragmented	Severely fragmented
Fiber arrangement	Compacted and parallel	Slightly loose and wavy	Moderately loose, wavy, and cross to each other	No identifiable pattern
Rounding of the nuclei	Long spindle shape cell	Slightly rounding	Moderately rounding	Severely rounding
Inflammation (area infiltrated by inflammation cell)	<10%	10%–20%	20%–30%	>30%

the most suitable condition to induce the tendon-related genes (Supplemental Figure 5). Although histological evaluation of these bio-tendons by hematoxylin and eosin (H&E) and Elastica van Gieson (EVG) staining showed no significant differences (Figure 2(b) and (c)), analysis by scanning electron microscopy (SEM) revealed regularly oriented collagen fibers aligned in the stretch direction in Mxk-iPSC-MSC-derived bio-tendons (Mxk-bio-tendons) (Figure 2(d)). The fibril direction in GFP-iPSC-MSC-derived bio-tendons (GFP-bio-tendons) was tangled and not aligned according to the mechanical stretch. Thus, Mxk-iPSC-MSCs in the new stretching 3D chamber culturing system could create tendon-like structures and showed aligned collagen fibers.

### *Decellularization and chemical cross-linking of the bio-tendon*

To exclude immune reactions and the risk of tumorigenesis related to the use of allogeneic human iPSC cells, we decellularized the created bio-tendons. We used high-pressure treatment, an established approach for tissue transplantation.<sup>29</sup> After decellularization, the cells were treated with DNase to reduce nucleic acid-dependent inflammation.<sup>30</sup> Histological analysis by H&E and 4',6-diamidino-2-phenylindole (DAPI) staining confirmed the complete nucleus depletion after decellularization and DNase treatment (Figure 2(e)).

To strengthen the mechanical properties of tissues for transplantation,<sup>31,32</sup> chemical cross-linking could be effective.<sup>33</sup> Here, chemical cross-linking was performed with N-ethyl-N-(3-(dimethylamino)propyl) carbodiimide/N-hydroxysuccinimide (EDC/NHS) to strengthen the mechanical properties of the bio-tendons. We analyzed the mechanical capacity of these bio-tendons and observed that the tensile strength of Mxk-bio-tendons was higher than that of GFP-bio-tendons, and that Mxk-bio-tendons had a higher stiffness/Young's modulus and lower failure strain (Figure 3).

### *Early infiltration of tenocyte-like cells into the Mxk-bio-tendon in transplantation models*

To test their performance in tendon reconstruction, we planted the designed bio-tendons into an Achilles tendon transplantation model<sup>34</sup> of mTmG mice<sup>35</sup> expressing

tdTomato fluorescence on all cell membranes. Six weeks after the transplantation, both Mxk and GFP bio-tendons were completely engrafted (Figure 4(a)). H&E and EVG stainings of the transplanted tendon were performed at 2 and 6 weeks after transplantation, and red fluorescent protein (RFP)/DAPI staining was performed to evaluate the infiltration of mTmG mouse-derived cells. As *ex vivo* gelation did not create stable products to perform the transplant experiments, we alternatively injected pepsin-solubilized collagen gel between the gaps of the Achilles tendon. At 2 weeks after transplantation, the Mxk-bio-tendon transplantation group showed aligned collagen fiber structure and the GFP-bio-tendon transplantation and gel-transplanted groups showed thin fiber density and inconsistent fiber formation (Figure 4(b)). Considering the infiltrating cells in the implanted tissue, round nuclear cells such as inflammatory cells appeared in both Mxk- and GFP-bio-tendon groups, while spindle-shaped cells such as tendon cells were also observed in the transplanted Mxk-bio-tendons (Figure 4(b)).

Based on the established quantitative evaluation system of tendon pathology in terms of fiber structure, fiber arrangement, nuclear roundness, and inflammation<sup>21</sup> (Table 1), the scores for fiber structure and nuclear roundness were lower in the group transplanted with Mxk-bio-tendons than in the group transplanted with GFP-bio-tendons (Figure 4(c)). These observations suggest that the transplanted Mxk-bio-tendons have the potential to recruit tendon cells to reconstruct into transplanted bio-tendons even at 2 weeks.

### *Mxk-bio-tendon has properties similar to those of the normal tendon in transplant models*

In the histological evaluation at 6 weeks post-transplantation, we observed more enriched collagen fibers aligned in parallel in the Mxk-bio-tendon transplantation group than in the other groups and the Mxk-bio-tendon-transplanted tissue at 2 weeks (Figures 4(b) and 5(a)).

RFP/DAPI staining revealed several tendon cell-like spindle-shaped cells arranged in an order in Mxk-bio-tendon group (Figure 5(a)). In the quantitative evaluation of tendon pathology, the scores of fiber structure, nuclear roundness, and inflammation were significantly lower in Mxk-bio-tendon group than in GFP-bio-tendon group, and the scores for fiber structure and arrangement were

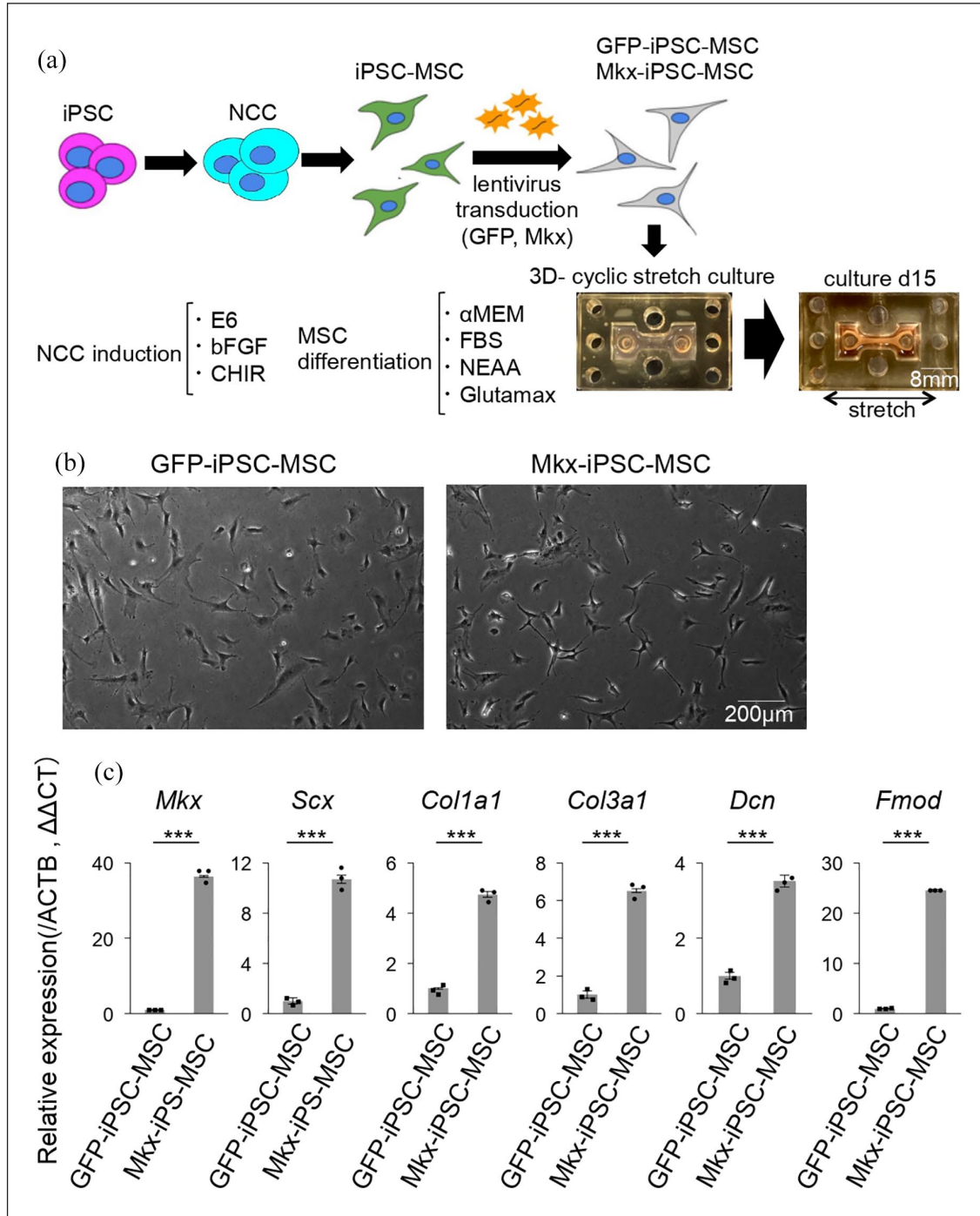


**Figure 1.** MSC induction from iPSCs. Mkx overexpression in iPSC-MSCs promoted tenogenic potential: (a) Schematic of the complete process of bio-tendon generation from iPSCs. First, we established NCCs with NCC induction media. The NCCs were then transferred into MSC differentiation media for further differentiation into MSCs. (b) Morphological changes in GFP-iPSC-MSCs and Mkx-iPSC-MSCs. (c) Quantitative PCR of GFP-iPSC-MSCs and Mkx-iPSC-MSCs ( $n=3$ ). ACTB as a reference. Mkx overexpression induced tendon-related gene expression. Student's  $t$ -test was used for statistical analysis. Data are represented as mean  $\pm$  SEM. \*\*\* $p < 0.001$ .

significantly lower in Mkx-bio-tendon group than in the gel-transplanted group (Figure 5(b)). Thus, the transplanted Mkx-bio-tendons more efficiently recruited tendon cells for the reconstruction process, which was not

observed in fibrotic scar-like tissue, at 6 weeks than at 2 weeks.

To evaluate the mechanical properties of the tendons reconstructed by bio-tendon transplantation, each group of

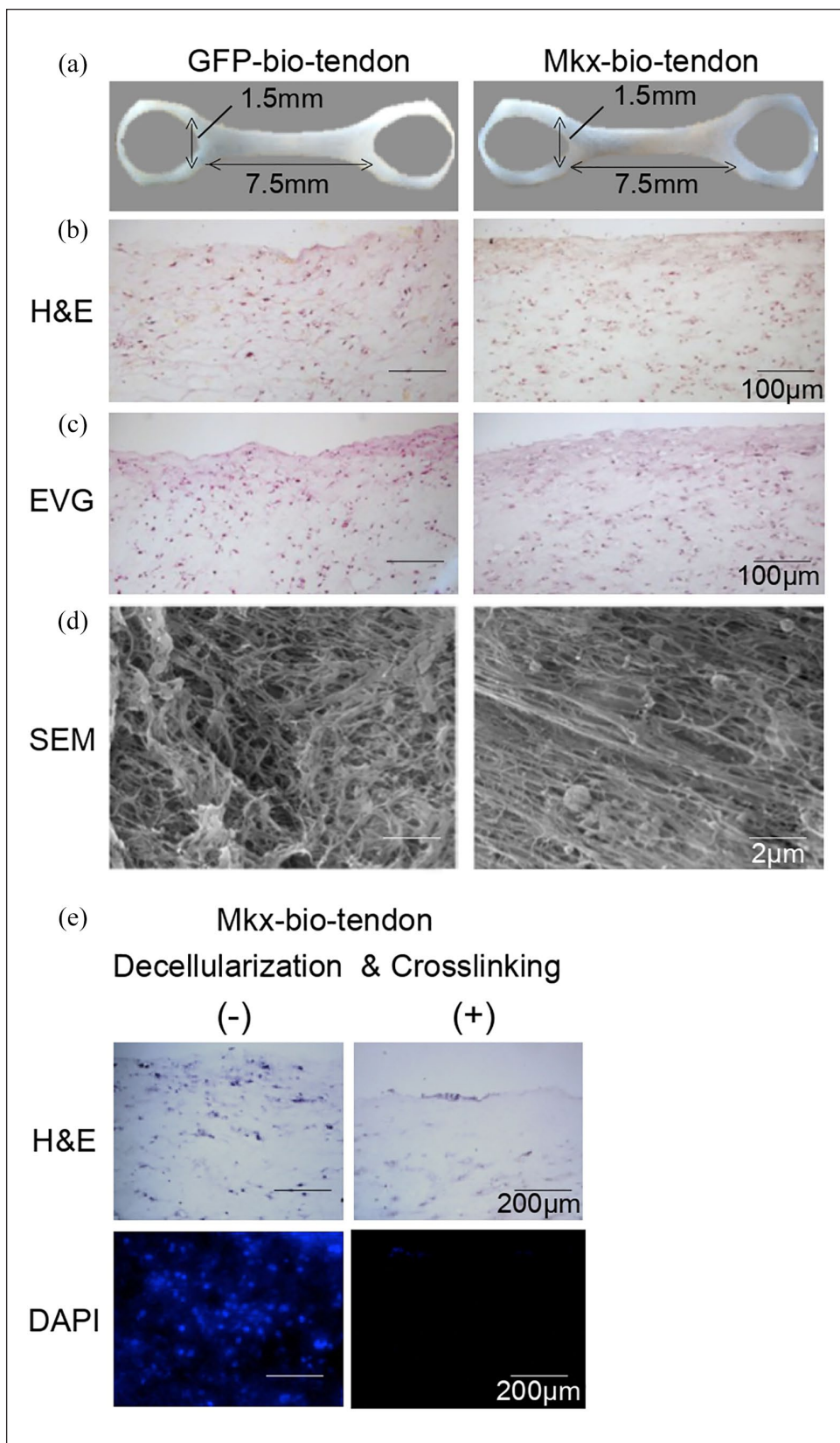


**Figure 2.** Combination of newly designed chamber and cyclic stretch with iPSC-MSCs could produce bio-tendons: (a) Comparison of bio-tendons generated from GFP-iPSC-MSCs and Mkx-iPSC-MSCs. (b and c) Histological analysis of each bio-tendon. Representative micrographs of H&E-stained tissue sections (b) and EVG-stained tissue (c) sections. (d) SEM images of the surface layer of GFP-bio-tendon and Mkx-bio-tendon. (e) H&E and DAPI staining of bio-tendon with or without treatment.

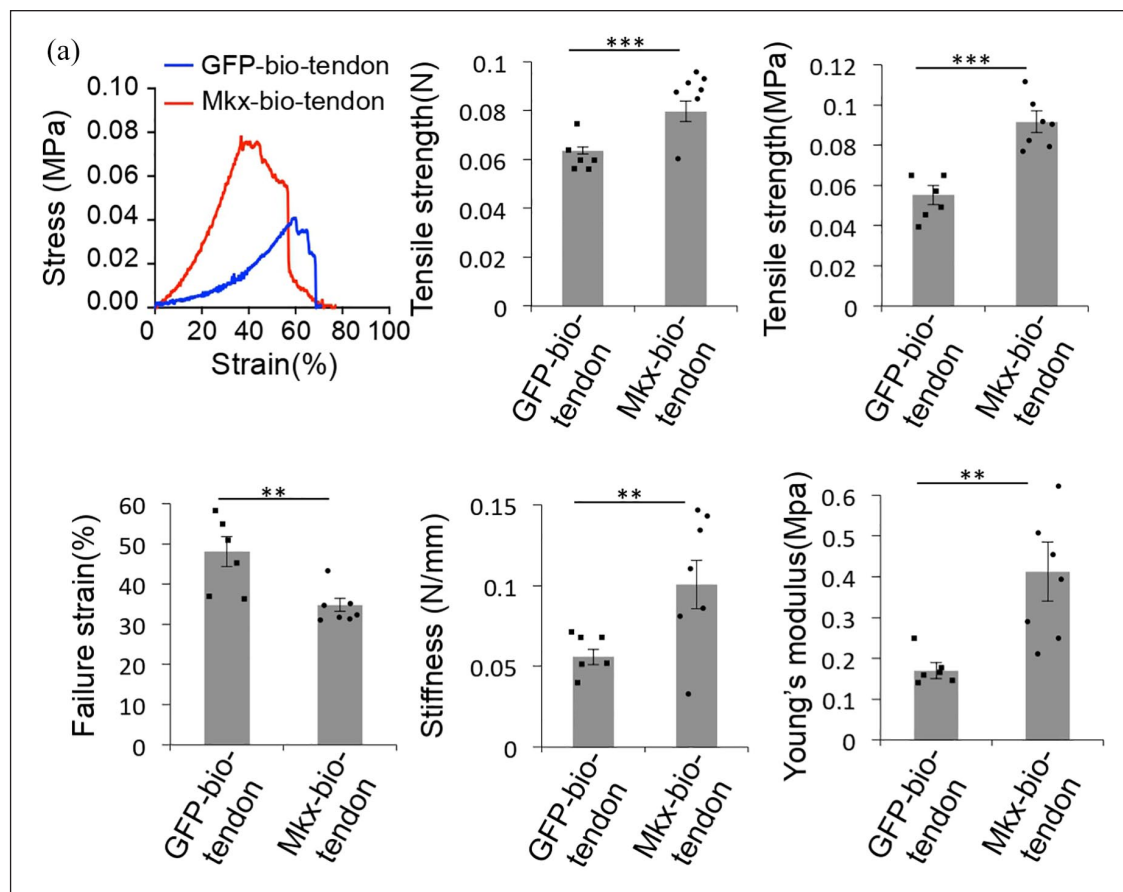


**Figure 3.** Mkk-bio-tendon had higher physical capacity. Strain curve and tensile strength of each bio-tendon after decellularization and cross-linking Student's *t*-test was used for statistical analysis. Data are represented as mean  $\pm$  SEM. \*\*\**p* < 0.001, \*\**p* < 0.01.

tendons was subjected to tensile tests 6 weeks after transplantation. The breakpoint was in the middle of the constructs, indicating that we could measure the physical capacity of the implanted bio-tendon. The tensile strength of Mkk-bio-tendon was comparable to that of the control normal tendon (Figure 6). The Young's modulus of Mkk-bio-tendon was also comparable to that of the control normal tendon, while that of GFP-bio-tendon and gel-transplanted control were lower (Figure 6). Taken together, these results indicate that Mkk-bio-tendon improved tendon reconstruction both histologically and biomechanically, which supports its capacity to promote physiological tendon regeneration and reconstruction.

## Discussion

The bio-tendons created in this study have several advantages for medical applications, including sufficient supply of human tendon-like cells for tissue generation. So far, there have been few reports on creation of artificial tendon-like tissues from human iPSCs and testing their capacity in animal models. Human iPSCs serve as a powerful tool to produce abundant mesenchymal stem cells that can differentiate

into tendon cells upon induction of *Mkx* expression, a master transcription factor for tendon cell differentiation.<sup>36,37</sup>

Previous reports have shown that *Mkx* expression is induced by mechano-stimuli in tendon cells,<sup>38,39</sup> and over-expression of *Mkx* in mesenchymal stem cells increases the expression of tendon-related genes.<sup>23,24</sup> Tendon cells differentiated by *Mkx* have the capacity to construct tendon-like tissues where collagen fiber alignment is well organized in response to mechano-stimuli produced by the 3D cell stretch incubation system.<sup>14</sup> Consistent with this finding, human iPSC-derived tendon-like cells could also create tendon-like tissues in which collagen fibers are oriented in the direction of the stretching stimuli. The newly designed 3D cell stretching chamber system significantly improved the size of the tendon-like tissue. This stretching chamber with pins, unlike a static chamber,<sup>40</sup> can transmit mechanical load to tendon cells, a phenomenon that is critical for tendon-like tissue formation.

Several groups have reported improvement in tendon injuries by direct transplantation of iPSC-derived tendon-like cells,<sup>41,42</sup> however, application of autologous iPSCs takes a long time in the clinical setting and cannot exclude tumorigenicity.<sup>23</sup> In the case of allogeneic iPSC application,

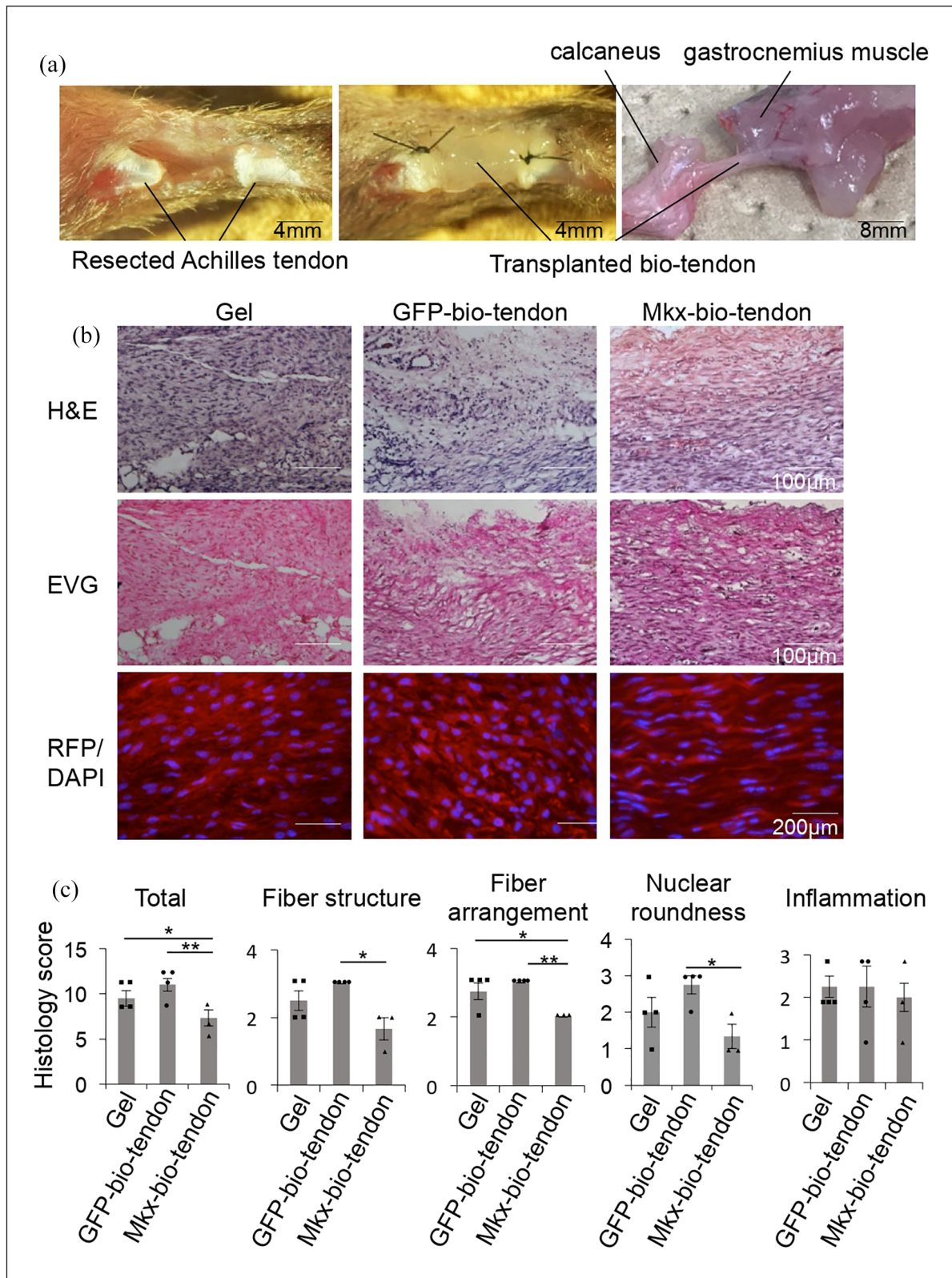


**Figure 4.** Transplantation experiment into mouse Achilles tendon and post 2-week assessment: (a) Images of mouse Achilles tendon transplant experiment. Six weeks after transplantation, the implanted Mkx-bio-tendons seemed to completely connect between the gastrocnemius muscle and ankle, suggesting engraftment. (b) Histological and immunohistochemical (IHC) analysis of 2-week post-transplant samples. See Supplemental Figures 3 to 5. (c) Histology scores. Three sections from each sample were randomly selected and three different fields in each section were analyzed by two blinded observers ( $n=3-4$ ). Tukey-Kramer test was used for statistical analysis. Data are represented as mean  $\pm$  SEM.  $^{**}p < 0.01$ ,  $^{*}p < 0.5$ . See Table 1.

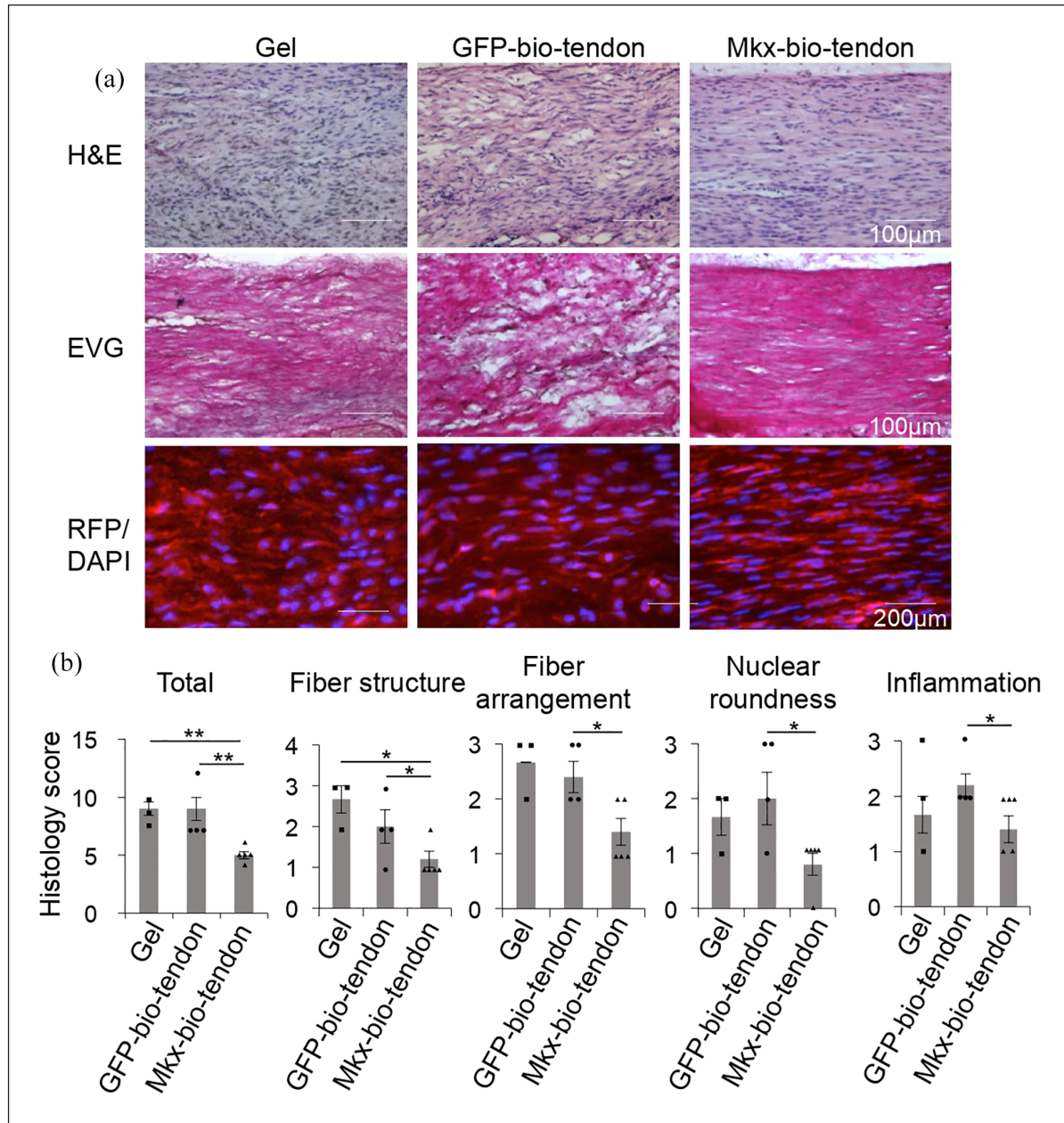


**Figure 5.** Assessment of 6-week post-transplant samples: (a) Histological and IHC analyses of 6-week post-transplant samples. (b) Histology scores. The analysis was performed as reported in Figure 3(c) ( $n=3-5$ ). Tukey-Kramer test was used for statistical analysis. Data are represented as mean  $\pm$  SEM. \* $p < 0.05$ . See Table I.

immunogenicity related to human leukocyte antigen mismatch should be considered.<sup>43</sup>

In this regard, the second advantage of our strategy is that the bio-tendons derived from human iPSCs are decellularized before transplantation. The advantage of decellularization of tendon tissues for transplantation has been well established in the application of allogeneic and xenogeneic tendon tissues; however, these tissues have several limitations such as shortage of supply and risk of infection or allergy. Bio-tendons could overcome these problems. For future clinical application of bio-tendons,

we should examine their capacity as a biomaterial using large animals.

The transplantation of Mkx-bio-tendon led to significantly improved therapeutic effects as compared to GFP-bio-tendon transplantation at 6 weeks after transplantation, including histologically well-aligned fiber structures and mechanical properties comparable to those of normal tissues.

In the reconstruction process after tendon transplantation, immune cell infiltration in the early stages was followed by mesenchymal cell migration. These cells could be differentiated into tendon cells.<sup>8</sup> Consistent with this

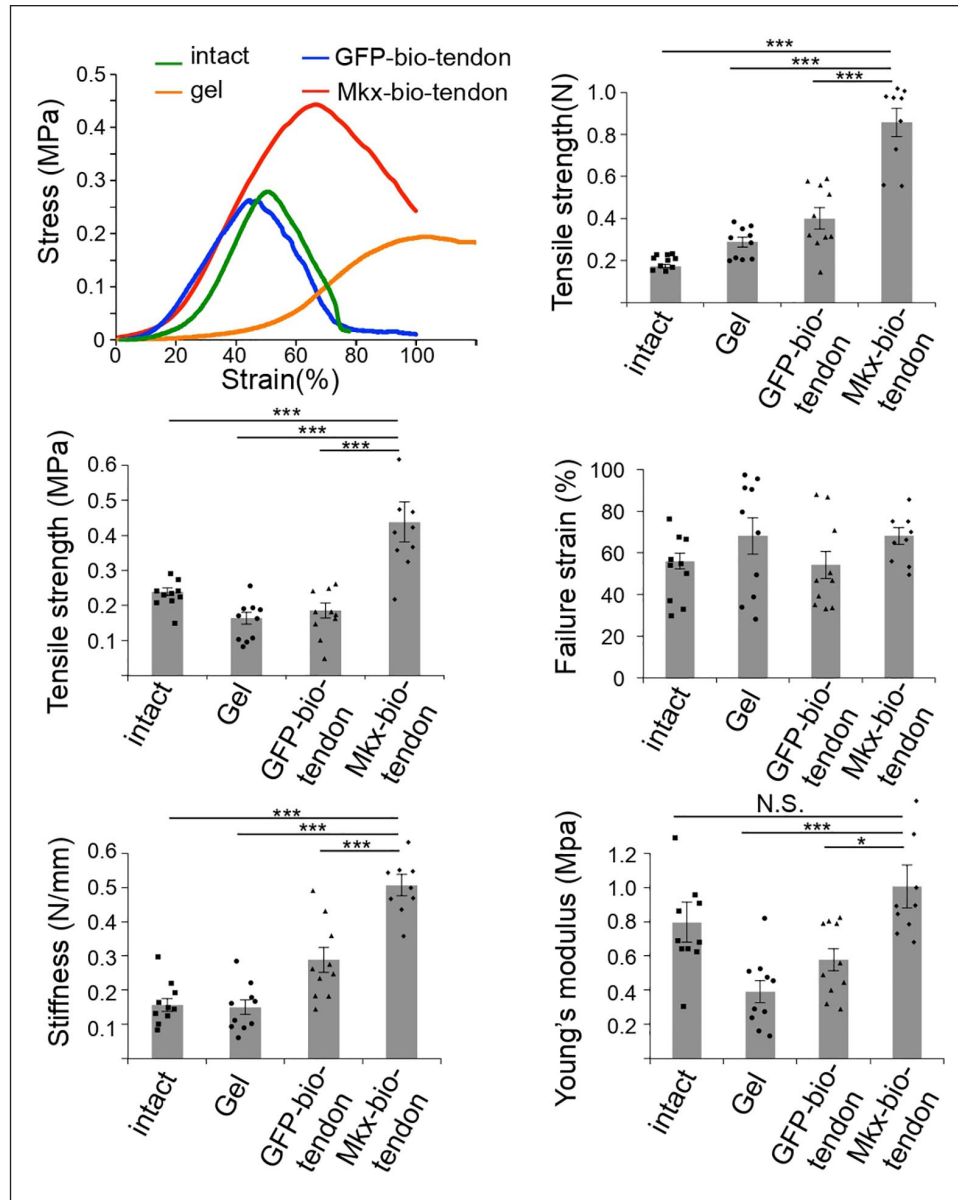


**Figure 6.** Mkx-bio-tendon induced biomechanically improved tendon reconstruction. Tensile strength of implanted bio-tendons (intact, gel, GFP-bio-tendon:  $n = 10$ , Mkx-bio-tendon:  $n = 9$ ). Six weeks after transplantation, we dissected the complex of the gastrocnemius muscle, implanted bio-tendon, and calcaneus (see Figure 4(a)) and measured the tensile strength of the implanted bio-tendon. Tukey-Kramer test was used for statistical analysis. Data are represented as mean  $\pm$  SEM. \*\*\* $p < 0.001$ , \* $p < 0.05$ , N.S., not significant.

finding, we observed inflammatory cell infiltration into both types of transplanted bio-tendons at 2 weeks, and spindle-shaped cells became dominant in the Mkx-bio-tendon but not in the GFP-bio-tendon samples at 6 weeks. The extracellular matrix (ECM) structure in transplanted decellularized tissues has been reported to play a critical role in stem cell differentiation,<sup>44</sup> supporting the idea that the well-aligned collagen fiber structure in Mkx-bio-tendons may promote proper recruitment of tendon progenitor cells and facilitate tendon cell differentiation to reconstruct tendon tissues.

Secreted proteins may also play a key role in the reconstruction, after tendon transplantation. In this study, we did not investigate the profiles of secreted proteins, such as growth factors. We might find therapeutic targets for improving regeneration by examining protein expression within implanted tissue, especially in Mkx-bio-tendon transplanted samples.

A limitation of the current approach is that we utilized collagen gel from porcine tendons. However, we cannot deny the possibility that this may provoke an immune reaction. Ideally, we should use human-derived collagen gel to completely

eliminate immunogenicity. Also, Mxk-bio-tendons do not have a physiological hierarchical structure observed in normal tendons. Physiological cross-linking via lysyl oxidase may not be well capitulated, leading to low tensile strength<sup>45</sup> that should be reinforced by chemical cross-linking. However, chemical cross-linking may be detrimental to viscoelastic properties. For future analysis, it is necessary to create biologically mimicking bio-tendons with physical and viscoelastic properties. These issues should be resolved through further renovation in the present bio-tendon generation protocol.

In summary, the Mxk-bio-tendon is a promising strategy for future clinical applications in tendon injury and diseases.

### Acknowledgements

We thank all the members of the Department of Systems BioMedicine at Tokyo Medical and Dental University for their support.

### Author contributions

Conceptualization, H.T., R.K., and H.A.; Methodology, H.T., R.K., T.C., and H.A.; Formal analysis, H.T., R.K., Y.F., and R.N.; Investigation, H.T.; Resources, R.S., K.S., T.K., T.K., and A.K.; Writing—original draft, H.T.; Writing—review and editing, R.K., Y.F., R.N., and H.A.; Funding Acquisition, H.A.; Supervision, H.A.

### Declaration of conflicting interests

The author(s) declared no potential conflicts of interest with respect to the research, authorship, and/or publication of this article.

### Funding

The author(s) disclosed receipt of the following financial support for the research, authorship, and/or publication of this article: This research was supported by AMED-CREST from the Japan Agency for Medical Research and Development (AMED) (JP21gm0810008 to H.A.) and JSPS KAKENHI (Grant numbers: 20H05696 to H.A.).

### ORCID iD

Hiroshi Asahara  <https://orcid.org/0000-0002-5215-8745>

### Supplemental material

Supplemental material for this article is available online.

### References

- Connizzo BK, Yannascoli SM and Soslowsky LJ. Structure-function relationships of postnatal tendon development: a parallel to healing. *Matrix Biol* 2013; 32: 106–116.
- Lin TW, Cardenas L and Soslowsky LJ. Biomechanics of tendon injury and repair. *J Biomech* 2004; 37: 865–877.
- Gulati V, Jaggard M, Al-Nammari SS, et al. Management of achilles tendon injury: a current concepts systematic review. *World J Orthop* 2015; 6: 380–386.
- Maffulli N, Via AG and Oliva F. Chronic achilles tendon rupture. *Open Orthop J* 2017; 11: 660–669.
- van den Boom NAC, Winters M, Haisma HJ, et al. Efficacy of stem cell therapy for tendon disorders: a systematic review. *Orthop J Sports Med* 2020; 8: 2325967120915857.
- Nourissat G, Berenbaum F and Duprez D. Tendon injury: from biology to tendon repair. *Nat Rev Rheumatol* 2015; 11: 223–233.
- Hardy A, Casabianca L, Andrieu K, et al. Complications following harvesting of patellar tendon or hamstring tendon grafts for anterior cruciate ligament reconstruction: systematic review of literature. *Orthop Traumatol Surg Res* 2017; 103: S245–S248.
- Cronce MJ, Faulknor RA, Pomerantseva I, et al. In vivo response to decellularized mesothelium scaffolds. *J Biomed Mater Res Part B Appl Biomater* 2018; 106: 716–725.
- Wong ML and Griffiths LG. Immunogenicity in xenogeneic scaffold generation: antigen removal vs. Decellularization. *Acta Biomater* 2014; 10: 1806–1816.
- Tulloch SJ, Devitt BM, Porter T, et al. Primary ACL reconstruction using the LARS device is associated with a high failure rate at minimum of 6-year follow-up. *Knee Surg Sports Traumatol Arthrosc* 2019; 27: 3626–3632.
- Sinagra ZP, Kop A, Pabbruwe M, et al. Foreign body reaction associated with artificial LARS ligaments: a retrieval study. *Orthop J Sports Med* 2018; 6: 2325967118811604.
- Terzi A, Gallo N, Bettini S, et al. Sub- and supramolecular X-ray characterization of engineered tissues from equine tendon, bovine dermis, and fish skin type-I collagen. *Macromol Biosci* 2020; 20: e2000017.
- Yin Z, Chen X, Zhu T, et al. The effect of decellularized matrices on human tendon stem/progenitor cell differentiation and tendon repair. *Acta Biomater* 2013; 9: 9317–9329.
- Kataoka K, Kurimoto R, Tsutsumi H, et al. In vitro neogenesis of tendon/ligament-like tissue by combination of Mohawk and a three-dimensional cyclic mechanical stretch culture system. *Front Cell Dev Biol* 2020; 8: 307.
- Winston TS, Suddhapas K, Wang C, et al. Serum-free manufacturing of mesenchymal stem cell tissue rings using human-induced pluripotent stem cells. *Stem Cells Int* 2019; 2019: 5654324.
- Izumi S, Otsuru S, Adachi N, et al. Control of glucose metabolism is important in tenogenic differentiation of progenitors derived from human injured tendons. *PLoS One* 2019; 14(3): e0213912.
- Ragni E, Perucca Orfei C, Bowles AC, et al. Reliable reference genes for gene expression assessment in tendon-derived cells under inflammatory and pro-fibrotic/healing stimuli. *Cells* 2019; 8(10): 1188.
- Dobin A, Davis CA, Schlesinger F, et al. STAR: ultrafast universal RNA-seq aligner. *Bioinformatics* 2013; 29(1): 15–21.
- Li B and Dewey CN. RSEM: accurate transcript quantification from RNA-Seq data with or without a reference genome. *BMC Bioinformatics* 2011; 12: 323.
- Ge SX, Son EW and Yao R. iDEP: an integrated web application for differential expression and pathway analysis of RNA-Seq data. *BMC Bioinformatics* 2018; 19: 534.
- Chen J, Yu Q, Wu B, et al. Autologous tenocyte therapy for experimental Achilles tendinopathy in a rabbit model. *Tissue Eng Part A* 2011; 17: 2037–2048.
- Faul F, Erdfelder E, Buchner A, et al. Statistical power analyses using G\*Power 3.1: tests for correlation and regression analyses. *Behav Res Methods* 2009; 41: 1149–1160.

23. Yamanaka S. Pluripotent stem cell-based cell therapy—promise and challenges. *Cell Stem Cell* 2020; 27: 523–531.
24. Nakamichi R, Ito Y, Inui M, et al. Mohawk promotes the maintenance and regeneration of the outer annulus fibrosus of intervertebral discs. *Nat Commun* 2016; 7(1): 12503.
25. Liu H, Zhang C, Zhu S, et al. Mohawk promotes the tenogenesis of mesenchymal stem cells through activation of the TGF $\beta$  signaling pathway. *Stem Cells* 2015; 33: 443–455.
26. Otabe K, Nakahara H, Hasegawa A, et al. Transcription factor Mohawk controls tenogenic differentiation of bone marrow mesenchymal stem cells in vitro and in vivo. *J Orthop Res* 2015; 33: 1–8.
27. Cserjesi P, Brown D, Ligon KL, et al. Scleraxis: a basic helix-loop-helix protein that prefigures skeletal formation during mouse embryogenesis. *Development* 1995; 121: 1099–1110.
28. Schweitzer R, Chyung JH, Murtaugh LC, et al. Analysis of the tendon cell fate using Scleraxis, a specific marker for tendons and ligaments. *Development* 2001; 128: 3855–3866.
29. Hashimoto Y, Funamoto S, Sasaki S, et al. Preparation and characterization of decellularized cornea using high-hydrostatic pressurization for corneal tissue engineering. *Biomaterials* 2010; 31: 3941–3948.
30. Crapo PM, Gilbert TW and Badylak SF. An overview of tissue and whole organ decellularization processes. *Biomaterials* 2011; 32: 3233–3243.
31. Juncosa-Melvin N, Shearn JT, Boivin GP, et al. Effects of mechanical stimulation on the biomechanics and histology of stem cell-collagen sponge constructs for rabbit patellar tendon repair. *Tissue Eng* 2006; 12: 2291–2300.
32. Nirmalanandhan VS, Rao M, Shearn JT, et al. Effect of scaffold material, construct length and mechanical stimulation on the in vitro stiffness of the engineered tendon construct. *J Biomech* 2008; 4: 1822–1828.
33. Makris EA, Responde DJ, Paschos NK, et al. Developing functional musculoskeletal tissues through hypoxia and lysyl oxidase-induced collagen cross-linking. *Proc Natl Acad Sci USA* 2014; 111: E4832–E4841.
34. Zantop T, Gilbert TW, Yoder MC, et al. Extracellular matrix scaffolds are repopulated by bone marrow-derived cells in a mouse model of achilles tendon reconstruction. *J Orthop Res* 2006; 24: 1299–1309.
35. Muzumdar MD, Tasic B, Miyamichi K, et al. A global double-fluorescent cre reporter mouse. *Genesis* 2007; 45: 593–605.
36. Ito Y, Toriuchi N, Yoshitaka T, et al. The Mohawk homeobox gene is a critical regulator of tendon differentiation. *Proc Natl Acad Sci USA* 2010; 107: 10538–10542.
37. Liu W, Watson SS, Lan Y, et al. The atypical homeodomain transcription factor Mohawk controls tendon morphogenesis. *Mol Cell Biol* 2010; 30: 4797–4807.
38. Suzuki H, Ito Y, Shinohara M, et al. Gene targeting of the transcription factor Mohawk in rats causes heterotopic ossification of Achilles tendon via failed tenogenesis. *Proc Natl Acad Sci USA* 2016; 113: 7840–7845.
39. Kayama T, Mori M, Ito Y, et al. Gtf2ird1-Dependent mohawk expression regulates mechanosensing properties of the tendon. *Mol Cell Biol* 2016; 36: 1297–1309.
40. Farhat YM, Al-Maliki AA, Chen T, et al. Gene expression analysis of the pleiotropic effects of TGF- $\beta$ 1 in an in vitro model of flexor tendon healing. *PLoS One* 2012; 7: e51411.
41. Komura S, Satake T, Goto A, et al. Induced pluripotent stem cell-derived tenocyte-like cells promote the regeneration of injured tendons in mice. *Sci Rep* 2020; 10: 3992.
42. Nakajima T, Nakahata A, Yamada N, et al. Grafting of iPS cell-derived tenocytes promotes motor function recovery after Achilles tendon rupture. *Nat Commun* 2021; 12: 5012.
43. Nakatsuji N, Nakajima F and Tokunaga K. HLA-haplotype banking and iPS cells. *Nat Biotechnol* 2008; 26: 739–740.
44. Guneta V, Zhou Z, Tan NS, et al. Recellularization of decellularized adipose tissue-derived stem cells: role of the cell-secreted extracellular matrix in cellular differentiation. *Biomater Sci* 2017; 6(1): 168–178.
45. Zeugolis DI, Paul GR and Attenburrow G. Cross-linking of extruded collagen Fibers—a biomimetic three-dimensional scaffold for tissue engineering applications. *J Biomed Mater Res* 2009; 89: 895–908.